Volume 17, Issue 3, 172522 (1-13)

Iranian Journal of Earth Science (IJES)

https://doi.org/10.57647/j.ijes.2025.16862

Microfacies analysis, depositional setting, and sequence stratigraphy of the Fahliyan Formation by integrating geological and petrophysical data on an oil field located in the Northwest of the Persian Gulf

Parynaz Rasouli Ghadi[1], Mehdi Sarfi[2,*], Mohsen Aleali[1], Zahra Maleki[1]

[1]*Department of Earth Sciences, Science and Research Branch, Islamic Azad University, Tehran, Iran.*
[2]*School of Earth Sciences, Damghan University, Damghan, Iran.*

[*]**Corresponding author:** m.sarfi@du.ac.ir

Original Research

Received:
6 April 2024
Revised:
17 June 2024
Accepted:
26 August 2024
Published online:
10 July 2025

Abstract:

Early Cretaceous Carbonates of the Fahliyan Formation are among the important reservoirs of the Persian Gulf. The findings of core description, thin section petrography, and petrophysical Gamma diagram from three key wells were used to 1) identify the facies, 2) interpret the depositional setting, and 3) analyze the sequence stratigraphy of the Fahlyian Formation. Twelve microfacies were identified and interpreted based on five categories of facies (i.e., the intertidal zone, lagoon, shoal, scattered reefs, and shallow open marine). The evidence of karstification and extensive facies alterations in the lower and upper boundaries reveal a significant unconformity in the Fahliyan Formation's basal sequence boundary. A Gamma diagram was used to assess the efficiency of dynamic integrated prediction error filter analysis (D-INPEFA) in identifying and matching depositional sequences. By calibrating the results of the boundaries which were determined by the D-INPEFA curve with the depositional sequences determined by petrographic investigations and the descriptions of the cores, it was revealed that positive breaks (PB) generally correspond to the sequence boundaries (SB). In contrast, negative boundaries (NB) are detected in association with maximum flood surfaces (MFS). Overall, comparing depositional sequences that were segregated using the findings of petrographic studies with the D-INPEFA Gamma diagram demonstrated that interpreting the depositional sequences based on data integration can provide valuable data in comprehensive reservoir investigations from a geological standpoint.

Keywords: Fahliyan formation; Persian Gulf; Facies; D-INPEFA; Sequence stratigraphy

1. Introduction

The identification of factors affecting the reservoir quality and determining the flow units are among the critical objectives in the comprehensive geological characterization of reservoirs (Ahr, 2008). Reservoir quality is a function of three interconnected parameters: 1) sedimentary facies, 2) diagenesis processes, and 3) tectonic developments. In this respect, sedimentary facies are the primary factors controlling rocks' geometry and pore structure. Nevertheless, many of the primary features of the pores typically change in carbonate reservoirs due to the significant influence of diagenesis (Hassan et al., 2022). Accordingly, sedimentary facies studies and the interpretation of the depositional setting are the fundamental components of the geological characterization of the reservoirs (Ahr, 2008). The components of hydrocarbon systems (e.g., source, reservoir, and cap rock) are generally distributed based on sequence stratigraphy patterns (Van Buchem et al., 2011). Sequence stratigraphic investigations can be performed using data from various scales, including microscopic thin sections, cores, petrophysical logs, and seismic profiles (Van Buchem et al., 2011; Kadkhodaie and Rezaee, 2017; Tavakoli, 2017; Yong et al., 2021; Jehangir Khan et al., 2021; Hassan et al., 2022; Rasouli Ghadi et al., 2022). Traditionally, precise and comprehensive insight into the depositional setting, facies evolutions, and stratigraphic sequence patterns is gathered

using data from the cores and microscopic thin sections. Nevertheless, cores are only available in a limited number of wells in discontinuous form due to the high cost, lengthy process, and the limits of their preparation (Hassan et al., 2022). Hence, it is essential to identify a method that, in conjunction with the core data, can provide a precise and continuous comprehension of the sequence stratigraphic framework at the well scale.

Petrophysical logs have long been used in sequence stratigraphic investigations (Catuneanu, 2006, 2017). The Gamma log has a low impact from environmental factors and is almost stable against diagenesis processes. Moreover, it is available in most wells drilled in a field. Therefore, it is employed effectively in identifying sequences and interpreting key sequence boundaries (Moghaddasi et al., 2020; Falahatkhah et al., 2021). A deeper understanding and data extraction has been made possible by employing a numerical interpretation of the Gamma log and calculating its consecutive diagrams (Falahatkhah et al., 2021). The curve of dynamic integrated prediction error filter analysis (D-INPEFA) is effective at identifying and matching sequence key boundaries (Behdad, 2019; Moghaddasi et al., 2020; Khalili et al., 2021; Yong et al., 2021; Kassem et al., 2022). In addition, the Gamma log is crucial for conducting sequence stratigraphic investigations as it enables sequence pattern presentation in every well drilled in a hydrocarbon field.

The present paper aims to identify the facies, interpret the sedimentary model, and identify the depositional sequences in the Fahliyan Formation, which is one of the significant hydrocarbon reservoir in the Northwestern section of the Persian Gulf. This research mainly focuses on examining the effectiveness of using Gamma log interpretation to identify and match critical sequence boundaries in the Fahliyan reservoir. The use of INPEFA diagram method for separating the depositional sequences is then verified by comparing the findings with the sequences determined by core data and thin section petrography.

2. Geological setting and stratigraphy

The Persian Gulf is a portion of the Tethys region that has witnessed significant tectonic events, including the opening and closure of the early, ancient, and Neo-Tethys. The Persian Gulf region was a portion of the Arabian Plate's passive margin from the Late Permian to the end of the Cretaceous (Sharland et al., 2001; Bahrehvar et al., 2021) (Fig. 1 (a)). The section studied in the present paper is located at the Kharg-Mish height, northwest of the Persian Gulf (Fig. 1(b)). Basement faults and the Zagros orogeny contributed to the field formation, an extended anticline with an N-NW slope. The uniform carbonate platform indicates that Middle Yamama, Upper Yamama, and Khami are the three informal divisions of the Fahliyan Formation in the study area. The Fahliyan Formation is 400 m thick, with the Surmeh Formation being the deepest Formation drilled in the studied field (Fig. 2 (a)). The studied field's Gamma log and the lithological column of the Fahliyan Formation's various informal areas (Middle Yamama, Upper Yamama, and Khami) are presented in Fig. 2 (b).

3. Materials and methods

The present study aims to investigate the facies characteristics, interpret the depositional setting, and distinguish the depositinal sequences of the Fahliyan Formation in one of the Persian Gulf's northwest fields (Table 1). These objectives were realized by integrating the findings from examining 499 m of the core, petrography of 664 microscopic thin sections, and typical petrophysical logs in three key wells (A, B, and C). All specimens were tainted with Alizarin Red S solution according to Dickson's method (Dickson, 1966) to determine their mineralogical composition (calcite separation from dolomite). All thin sections went through high-resolution scanning to obtain a general comprehension of the thin section alterations relative to the studied aspects. A scanner with an accuracy of up to 10000 DPI, courtesy of the Research Institute of Petroleum Industry was used to

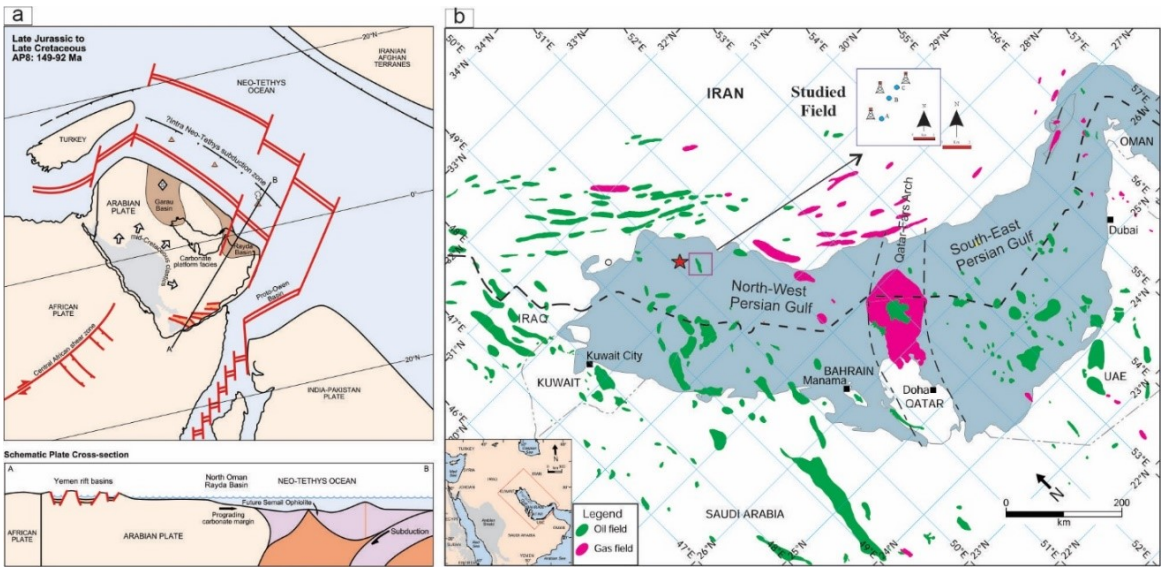

Figure 1. Upper Jurassic-Cretaceous paleogeography map of the Arabian Plate and surrounding areas (Sharland et al., 2001); the investigated field and three key wells' locations in the northwestern Persian Gulf are shown in the map (Modified from Al-Husseini (2007)).

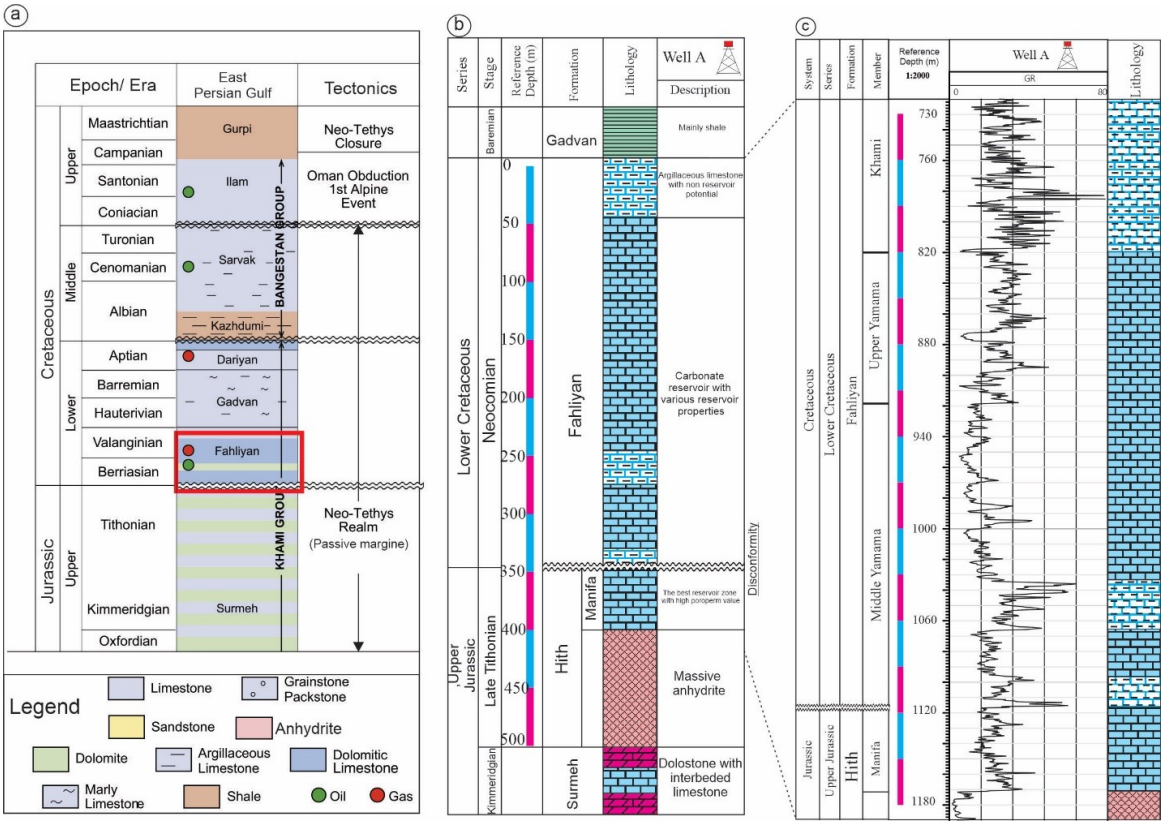

Figure 2. The stratigraphic column and lithological characteristics of the Surmeh, Hith, Fahlian, and Gadvan formations in key well A demonstrate that the Jurassic-Cretaceous boundary discontinuity develops at the boundary of the Hith and the Fahiyan Formation's Manifa carbonate succession. The stratigraphic column of the Fahlian Formation and the variations of the gamma log, informal subdivisions (Middle Yamama, Upper Yamama, and Khami) are depicted in key well A.

undertake the scanning process. Petrography data from thin sections and core descriptions were assembled to identify and separate facies. Afterward, a sedimentary model for the Fahliyan Formation in the studied field was constracted based on the relationship between the facies, their characteristics, and the presence or absence of reef-forming facies. Due to the significance of the unconformity at the base of the Fahliyan Formation for interpreting sequence stratigraphy, this sequence boundary was interpreted using the facies and diagenesis evidence. Eventually, the model proposed by Van Wagoner et al. (1990) was applied to identify the sequences and provide a framework for sequence stratigraphy. A depositional sequence is presented based on this model and a combination of the transgressive system tract (TST) and the high-stand system tract (HST) by identifying the sequence boundaries and the specified maximum flooding surface (MFS). The findings of this method were then compared with the sequences identified through cores and thin sections to assess the efficiency of the D-INPEFA Gamma log in separating sequences and key boundaries. Finally, the aforementioned method's efficiency is determined based on the correspondence of the specified key boundaries interpreted through the D-INPEFA Gamma log with the real sequences.

4. Results and discussion

4.1 Sedimentary facies and depositional setting

Sedimentary texture, grain size, type and abundance of allochems, fossils content, and other sedimentary parameters were interpreted using petrography of microscopic thin sections and cores description. The aforementioned data and their interpretations, comparisons with standard models, and a number of previous investigations on the Fahliyan Formation (e.g., Flugel (2010); Adabi et al. (2010); Jamalian et al. (2011); Noori et al. (2019); Esrafili-Dizaji et al. (2020); Bahrehvar et al. (2021); Hosseini et al. (2021)

Table 1. Data from the investigated field in the northwest of Persian Gulf.

Well	Core thickness (m)	Thin sections	Typical petrophysical logs
A	70	205	Available
B	178	248	Available
C	251	211	Available
Total	499	664	Three wells

resulted to recognition of eight facies in the Fahliyan Formation. There is clear evidence for the recorded facies in cores and petrographic descriptions of microscopic thin sections (Figs. 3 and 4). Moreover, allochems including the calcareous algae fragments, bivalves, corals, bryozoans, benthic foraminifera, gastropods, echinoderms, and sponge spicules are the skeletal components of the Fahliyan Formation. The most common non-skeletal components include ooids, peloids, intraclasts, and oncoids. These facies are concisely characterized and interpreted in the following sections.

4.1.1 Shallow open marine

Sponge spicule-echinoderm mudstone-wackestone (F1): This facies is characterized by the abundance of sponge spicules (approximately 10%) and echinoderm fragments (approximately 5%) (Figs. 3 (a-1) and 3 (a-2)). The abundance of echinoderm fragments, sponge spicules, bivalves, some benthic foraminifera, and dispersed pyrite crystals demonstrate the deposition of this facies in a shallow open sea environment (Flugel, 2010).

4.1.2 Dispersed patch reefs and shoal

Lithocodium boundstone facies (F2): the facies are characterized by a 5% abundance of Lithocodium algae and further skeletal components such as benthic foraminifera, bivalves, and gastropods with 5% abundance inside a boundstone texture (Figs. 3 (b-1) and 3 (b-2)). Peloid and intraclast are the most important non-skeletal components of this facies. Lithocodium algae commonly form patch reefs and cannot be regarded as barrier reef-forming components (Flugel, 2010). Both the platform's edge and the lagoon environment are suitable for developing patch reefs of the Fahliyan Formation (Esrafili-Dizaji et al., 2020).
Oncoid grainstone facies (F3): The primary components of this facies are Lithocodium algae and oncoids, which account for about 32% of the rock composition. With a frequency of around 7%, the intraclast is another subordinate component of this facies (Figs. 3 (c-1) and 3 (c-2)). The abundance of sizable oncoids with a diameter of approximately 1.5 cm indicates the developments of this facies on the shoal's platform edge sub-environment and its seaward portion. Moreover, the aforementioned environment has

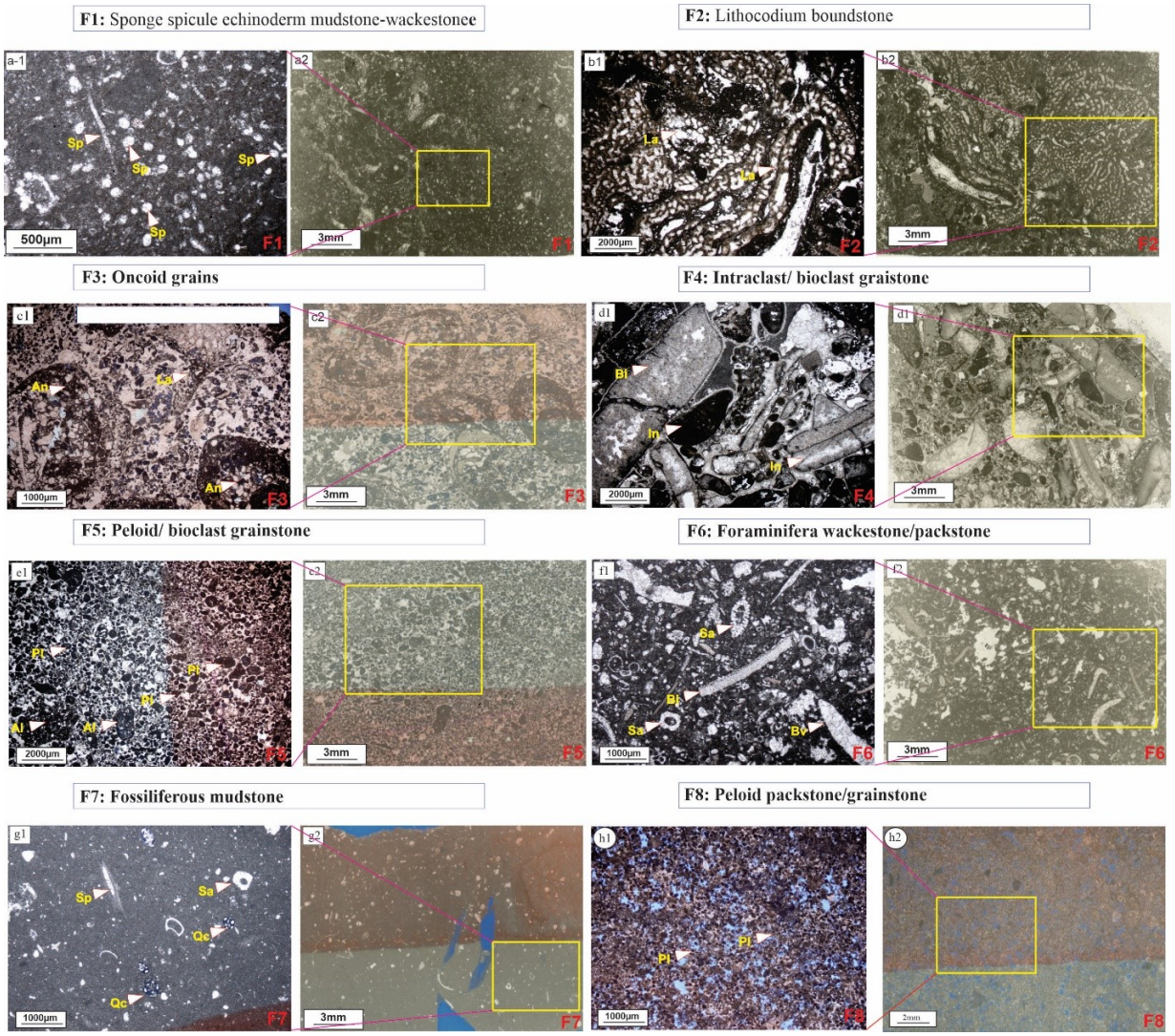

Figure 3. Microscopic thin-section images and their scans of eight main facies observed in the Fahliyan Formation in the northwestern section of the Persian Gulf.

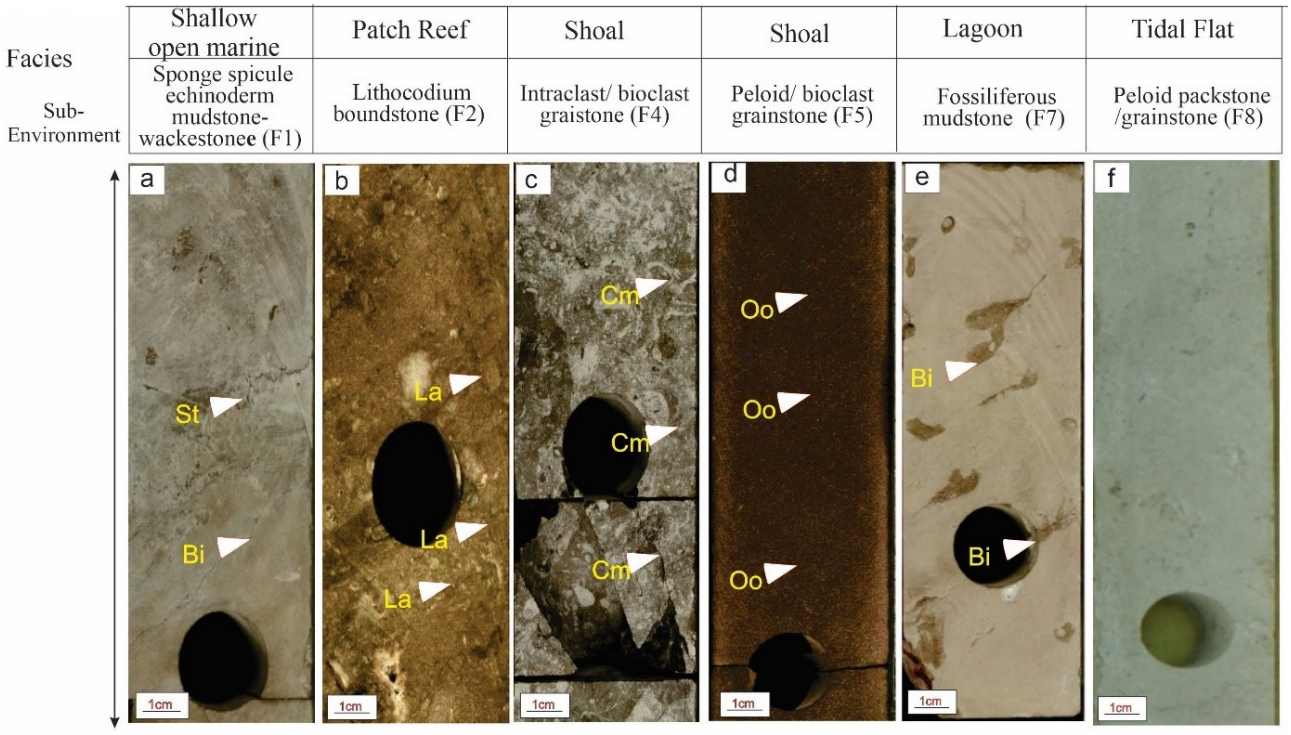

Figure 4. Images of the core sections of the sub-environments recognized in the Doroud Fahliyan Formation: (a) Grainstones related to the sub-environment of the intertidal zone; (b) Mudstone-wackestones related to the lagoon sub-environment; (c) Bioclastic packstone containing abundant algae associated with the lagoon sub-environment; (d) Ooid-peloid grainstone associated with the shoal sub-environment; (e) Algal rudstone related to dispersed reefs; (f) Echinoderm-bearing wackestone-packstone in sub-environment of shallow open marine (Bi: bioturbation, Cm: cementation, Bo: bioclast, Oo: ooid, An: oncoid, La: Lithocodium alga, St: stylolite).

had adequate water circulation (Esrafili-Dizaji et al., 2020). Bioclast-intraclast grainstone facies (F4): This facies comprise skeletal components include algae and bivalves (35%) and intraclast (15%). The constituents of this facies are angular and similar to the rudite in size (Figs. 3 (d-1) and 3 (d-2)). The abundance of skeletal and non-skeletal components indicates the deposition of this facies in a shoal environment with adequate water circulation.

Peloid/bioclast grainstone facies (F5): The dominant skeletal components in these facies include bivalves, benthic foraminifera, gastropods, sponge spicules, and green algae incorporated in a packstone texture (Figs. 3 (e-1) and 3 (e-2)). The micritization and bioturbation of this facies can be attributed to the presence of peloids, which are the most important non-skeletal components. The calcite cement deposit has filled the skeletal areas primarily with drusy fabric. This fabric is generated due to the aragonite composition of the skeletal areas after dissolution, primarily caused by meteoric diagenesis.

4.1.3 Lagoon

Foraminiferous wackestone-packstone facies (F6): The dominant skeletal components in this facies include benthic foraminifera, bivalves, gastropods, sponge spicules, and green algae, incorporated in a packstone fabric (Figs. 3 (f-1) and 3 (f-2)). The micritization and bioturbation of this microfacies can be attributed to the presence of peloids, which are its most important non-skeletal components. The calcite cement has filled the skeletal areas primarily with drusy fabric. This fabric is generated due to the aragonite composition of the skeletal areas after dissolution, primarily caused by meteoric diagenesis.

Fossiliferous mudstone facies (F7): This facies is characterized by a high abundance of small benthic foraminifera including miliolids, sponge spicules, and dispersed Salpingoporella algae with an abundance of approximately 15% (Figs. 3 (g-1) and 3 (g-2)). Bioturbation is the most significant characteristic found in the cores of this microfacies. The results show the occurrence of dolomitization along this structure. The lack of fossil diversity and the predominance of the mud texture indicate the deposition of this microfacies in an enclosed lagoon under extreme environmental stress (Flugel, 2010). The low diversity of fossils in the lagoon zone is due to the high environmental stress and salinity.

4.1.4 Intertidal zone

Peloid grainstone facies (F8): This facies is characterized by the approximate abundance of peloids at 15% and ooids at 20%. Micritization generally affects ooids, and their internal formation is often unknown (Figs. 3 (h-1) and 3 (h-2)). Moldic pores have formed due to the dissolution of certain ooid cores with aragonite composition. This facies have occasionally been found in conjunction with intertidal zone dolomites. Fig. 4 depicts core images of the identified facies aggregations in the Fahliyan Formation. Examining the microfacies and facies belts abundance reveals that the facies associated with the shoal sub-environment and patch reefs are the most prevalent and abundant (Fig. 5). In this study, a carbonated ramp platform was introduced for the

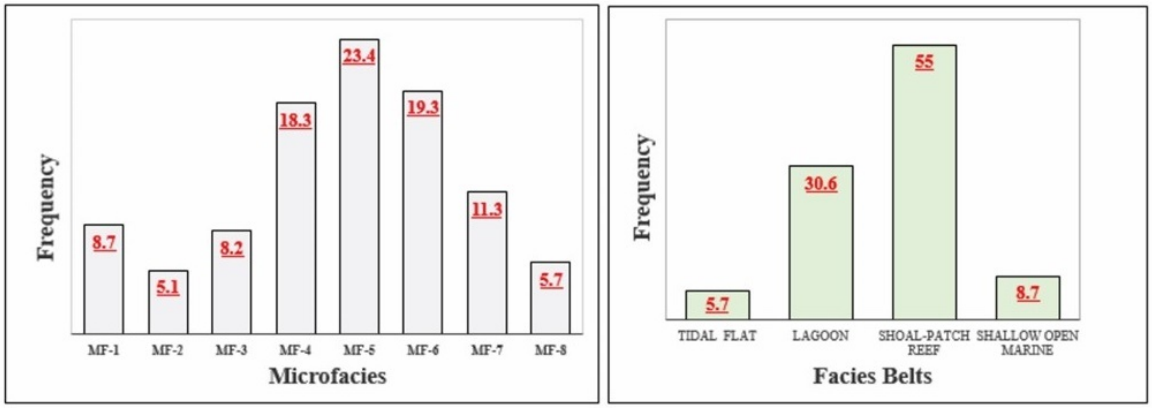

Figure 5. The abundance of facies and facies associations in the Fahliyan Formation of the investigated field; the findings demonstrate that shoal facies are the most abundant.

Fahliyan Formation, followed by representing the distribution of various microfacies (Fig. 6). This interpretation is based on the following factors: 1) the inadequacy of the development of reef-forming facies at the edge of the platform, 2) the absence of reworking by storms facies, and 3) the high abundance of grainstone facies. The previous literature has also assumed the deposition of the Fahliyan Formation in a carbonated ramp platform (Jamalian et al., 2011; Noori et al., 2019; Esrafili-Dizaji et al., 2020; Hosseini et al., 2021). In other words, Fahliyan Formation has been primarily deposited within a carbonated ramp in primarily energetic sub-environments.

4.2 Unconformity in the Jurassic–Cretaceous boundary

The regional studies of sequence stratigraphy in the Arabian Plate show that the unconformity separating large-scale sequences AP7 and AP8 has occurred at the upper boundary of the Hith and Gutnia formations (Sharland et al., 2001). The Manifa stromatolite-bearing carbonates are taken into account as the carbonated zones of the Hith Formation. This assumption is due to the findings of previous literature (Sharland et al., 2001; Hughes and Naji, 2008), the shallowness of the carbonated zones, scattering in the presence of evaporite types, their temporal position in the stratigraphic framework (Late Tithonian age), and being surrounded by an important unconformity surface at the Jurassic–Cretaceous boundary (Tithonian–Berriasian boundary) (Bahrehvar et al., 2021). In other words, the carbonate succession is the Hith Formation despite the lithological continuity of shallow stromatolite-bearing carbonates of Manifa with the Fahliyan Formation. In this regard, the Jurassic–Cretaceous boundary unconformity can be interpreted using core analysis, petrography of microscopic thin sections, and lithology (Fig. 7). The evidence for this unconformity includes karstification, the development of extensive pore porosity, size growth of bottlenecks in intergranular porosity, and the formation of meteoric cement. Extensive facies changes are evidenced at the Jurassic–Cretaceous boundary due to this unconformity event. Accordingly, the sub-environment wackestone facies of the shallow open marine immediately overlies the stromatolitic facies associated with the intertidal zone sub-environment. There is clear evidence of this unconformity

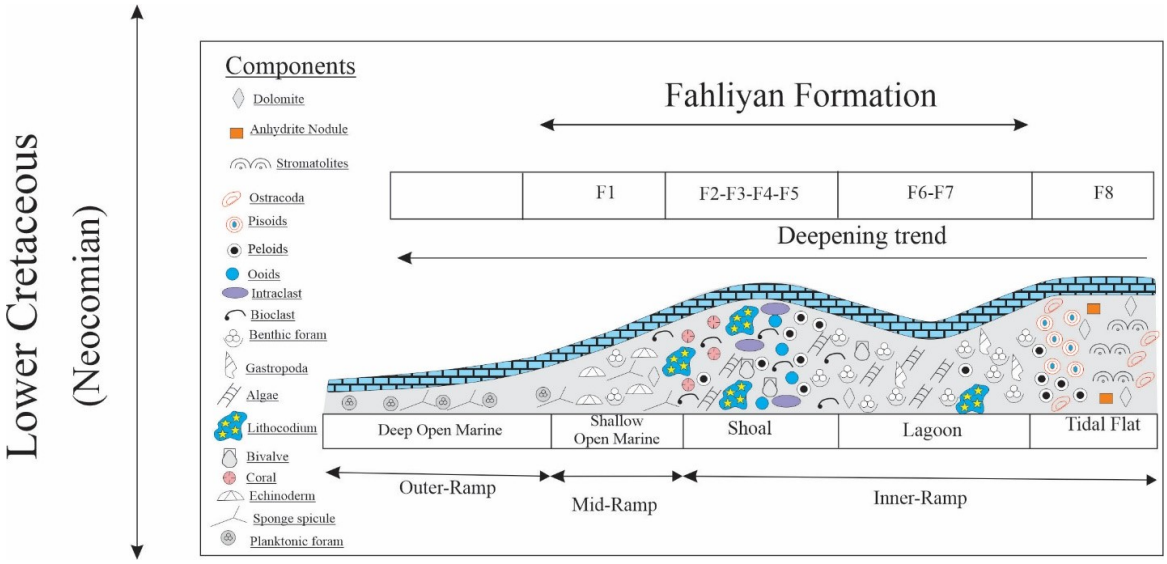

Figure 6. A schematic diagram of the sedimentary model of the carbonated ramp in the Fahliyan Formation in the studied field based on the facies distribution and their trend changes.

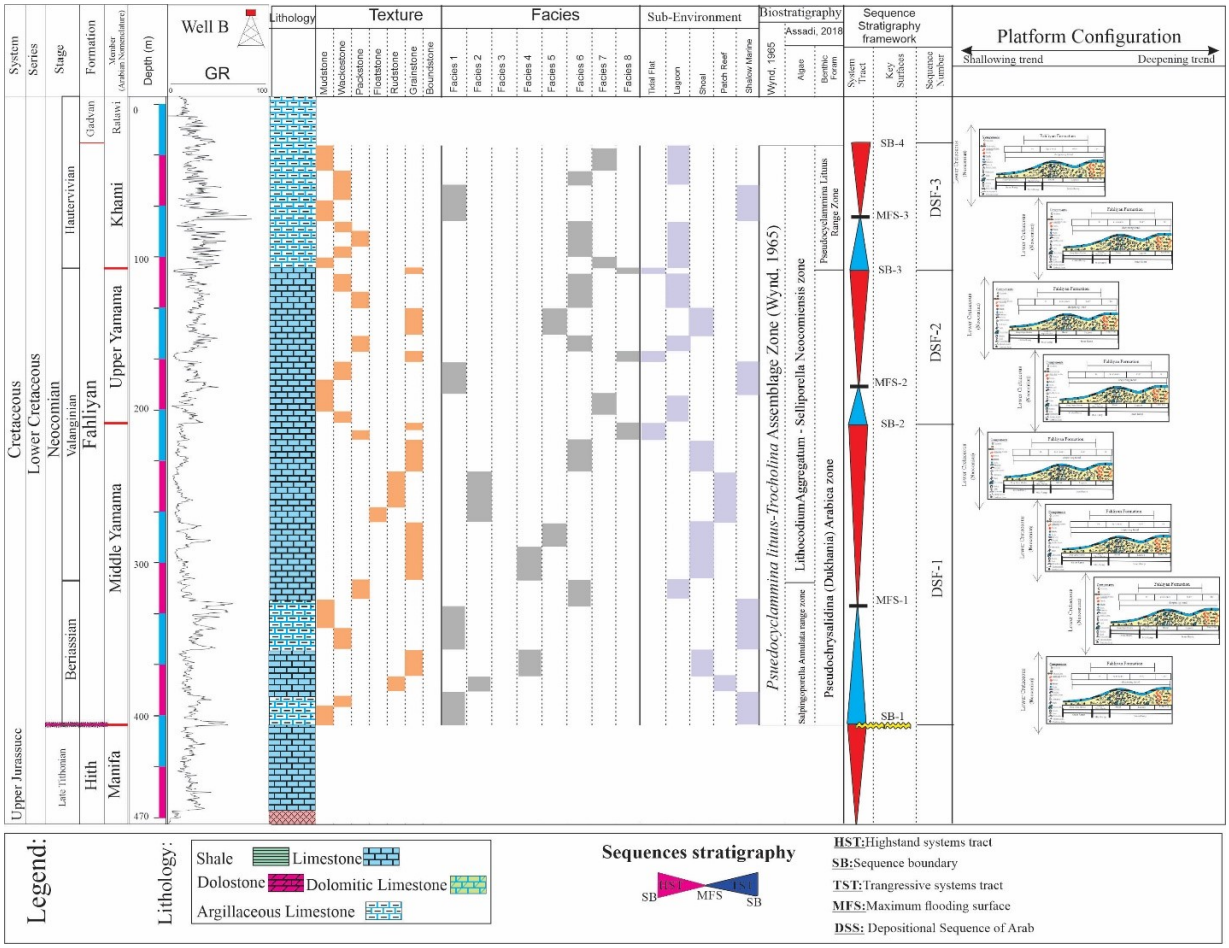

Figure 7. Lithostratigraphic log of the Fahliyan Formation in the northwestern section of the Persian Gulf; Note the changes in pattern in the depositional setting and the platform pattern and changes in the depositional sequences.

on cores and thin sections. Moreover, it can shift abruptly on common lithology logs with enhancing Gamma values and porosity reduction, particularly Gamma. The boundary separating the AP7 and AP8 large-scale sequences is believed to correspond to the Jurassic–Cretaceous boundary unconformity (Sharland et al., 2001; Bahrehvar et al., 2021). northwest of the Persian Gulf; clear evidence on cores, microscopic thin sections, and lithology charts identifies this unconformity as an essential and adaptive sequence boundary.

4.3 Sequence stratigraphy

The sequence stratigraphy framework of the Fahliyan Formation was identified using the patterns of vertical facies changes, facies type, particular depositional environment, and three third-order depositional sequences. The TST is commonly characterized by the development of lagoonal and open marine facies at the base. Moreover, the deepest shallow open marine facies matches the MFS. The HST, on the other hand, is commonly characterized by the development of grainstone shoal facies at the base and the intertidal zone facies at the top. Fig. 8 depicts/illustrate identifying depositional sequences in key well B2 and petrographic evidence of key sequence boundaries. A summary of the depositional sequence of the Fahliyan Formation is given in the following section.

Depositional Sequence 1 (DSF-1): This 220-m-thick sequence contains the middle Yamama subdivision of the Fahliyan Formation. The thickness of the TST and the HST is approximately 85 and 135 meters thick, respectively. The MFS (MFS-1) is determined using the facies maximum depth and the Gamma diagram's/log's high motif. This boundary may be equivalent to K10 (Sharland et al., 2001) in other sections of the Arabian Plate. The major development of grainstone facies characterizes this sequence. The unconformity of the Cretaceous–Tertiary boundary (the boundary of Fahliyan Formation and Manifa stromatolite-bearing carbonates) defines the sequence boundary at its base. Besides, evidence of karstification and the development of moldic porosity defines the upper boundary. In other words, both boundaries at the base and the top of this sequence are characterized by type 1 and indicate unconformity.

Depositional Sequence 2 (DSF-2): This sequence includes the upper Yamama subdivision of the Fahliyan Formation with a thickness of approximately 65 m. The thickness of TST and the HST is approximately 35 and 135 meters, respectively. The MFS is associated with the facies of shallow open marine. The development of shallow open marine facies and the high level of the gamma log are indicators of this MFS (MFS-2). In other sections of the Arabian Plate, this boundary may be equivalent to K20 (Sharland et al.,

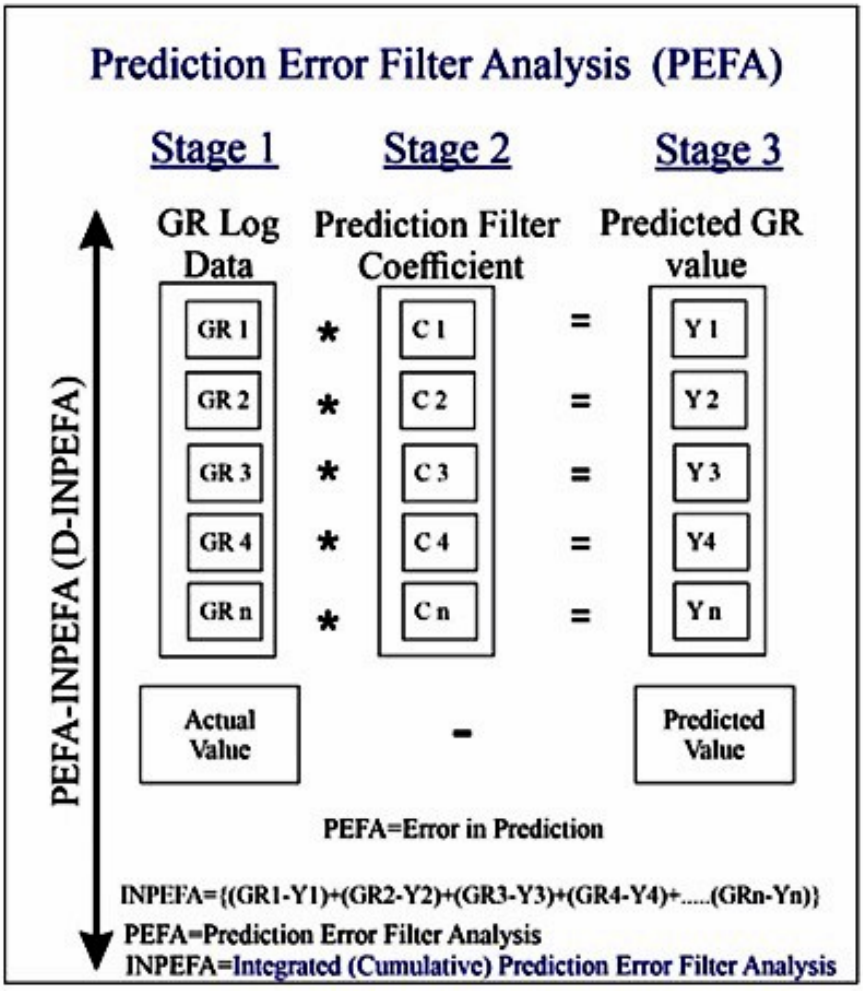

Figure 8. The process for calculating the PEFA and INPEFA; the cumulative error values of the PEFA log are represented by the INPEFA log (Nio et al., 2014). An instance of the values determined by this method is demonstrated in a part of Well A2.

2001). Unlike sequence 1, the major features of this sequence are the abundance of lagoonal facies and, to a lesser extent, open marine.

Depositional Sequence 3 (DSF-3): With a thickness of about 80 m, this sequence is restricted to the upper Khami subdivision of the Fahliyan Formation. The thickness of the TST and the HST is approximately 35 and 135 meters, respectively. These two boundaries are type two. The MFS (MFS-3) correlates to a sequence with a high Gamma level and is equivalent to K30 in other sections of the Arabian Plate (Sharland et al., 2001). Generally, sequence 3 acts as the cap rock for the Fahliyan reservoir by developing the dominant mud facies.

4.3.1 Gamma log and sequence stratigraphy

The Gamma diagram/log is among the essential petrophysical diagrams/log's applied to interpret the depositional setting and sequence stratigraphy. Two approaches are commonly used to interpret the depositional sequences based on the Gamma diagram/log: 1) the shape and changes trend of the Gamma diagram/log and 2) determining the changes and transformations of the sedimentary basin and sequence levels based on numerical values (Krassay, 1998; Nio et al., 2014; Tavakoli, 2017). The pattern of sediment deposition can be presented, and key sequence boundaries are determined based on the pattern of the Gamma diagram/log, which is commonly box-, bell-, funnel-, sawtooth, symmetrical-, and bow-shaped (Fig. 9) (Krassay, 1998). The Gamma deviation log (GDL) and the dynamic integrated prediction error filter analysis (D-INPEFA) are used along with the calculation charts introduced to separate the sequences. The following paragraphs provide a brief introduction to the D-INPEFA and NCGDL curve calculation methods and their use in key sequence boundary separation.

4.3.1.1. Dynamic integrated prediction error filter analysis method

The CycloLog® software is commonly used in sequence stratigraphic investigations to analyze petrophysical diagrams, particularly Gamma log (De Jong et al., 2006). Gamma log analysis is commonly applied to calculate PEFA and D-INPEFA logs. As a first step in determining the D-INPEFA diagram/log, the Gamma diagram/log is subjected to a PEFA. Next, Gamma values are determined in a depth range by employing a filter coefficient. The values of the predicted Gamma log are then determined by multiplying the Gamma values by the calculation coefficient. PEFA is a process to determine the error between the predicted actual and calculated Gamma values. In each 0.15 cm, these val-

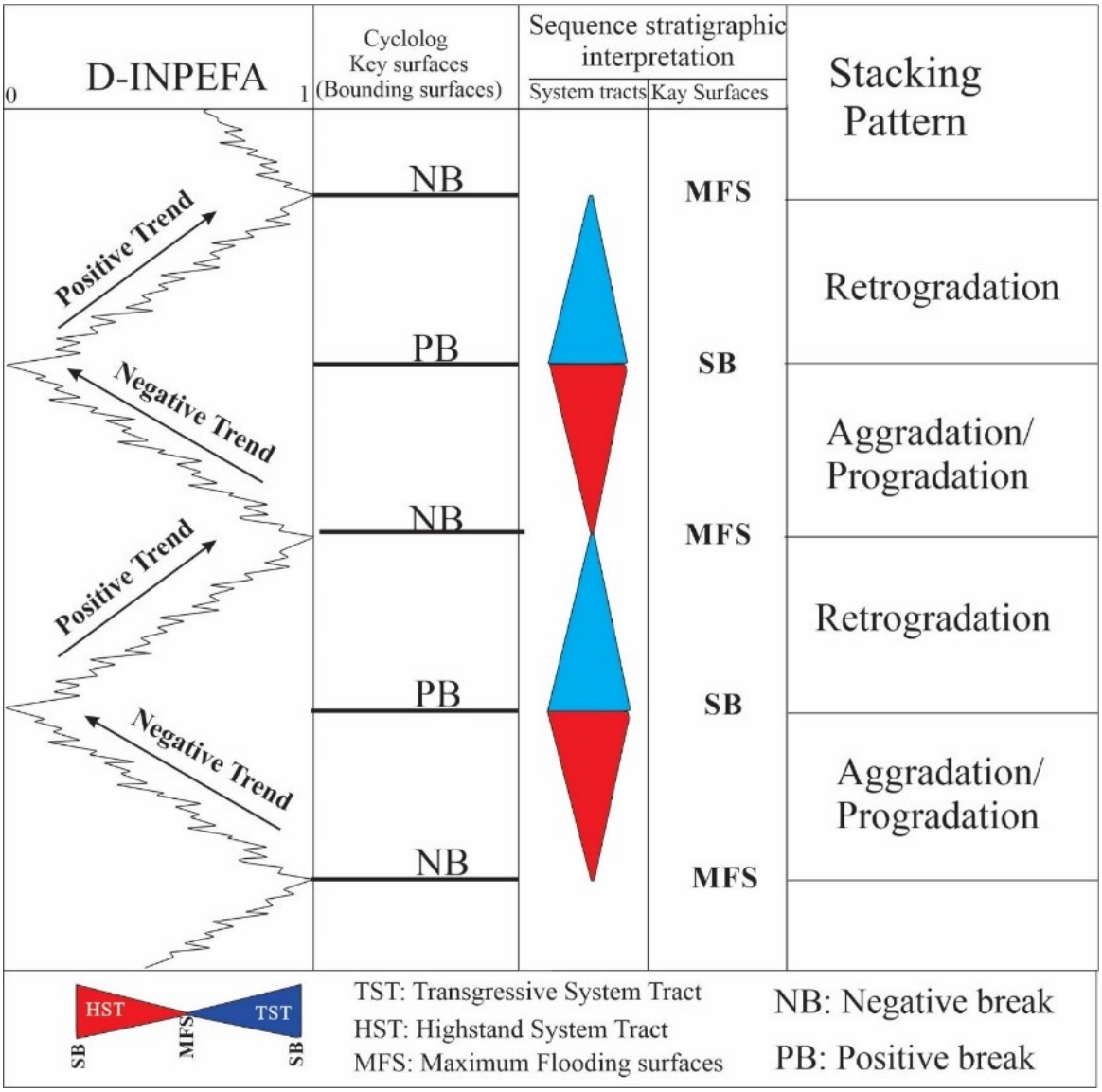

Figure 9. A schematic representation of the shifts in turning points of the D-INPEFA curve and key sequence stratigraphy stratal surfaces, such as sequence boundaries and maximum flood surfaces; Note the common shifts in sequence boundaries associated with the turning points of these curves. Some investigations may fail to detect this change process in some cases.

ues are recorded as a continuous log (log sampling interval). A different curve known as the D-INPEFA is developed cumulatively from this diagram because the PEFA curve does not adequately depict changes in the Gamma diagram, environmental settings, and Milankovitch cycles. The D-INPEFA or INPEFA logs presents cumulative error values showing the quantity of difference between the real and approximated values over time (De Jong et al., 2006). Fig. 8 illustrate the process of calculating PEFA and INPEFA logs (Nio et al. 2014). D-INPEFA is the dynamic mode of INPEFA log calculation. In other words, there is no significant difference between INPEFA and D-INPEFA logs because they show a similar concept.

Variations of positive (PB) and negative breaks (NB) in D-INPEFA values are between 0 and 1. The stratigraphic adaptation uses the curve's turning points, which identify the change process (Nio et al., 2014). According to the stratigraphic interpretation (Fig. 9), the PB boundaries correspond to the SB in most cases, while the NB boundaries correspond to the MFS (De Jong et al., 2006). However, it is essential to compare it with the core data and the sedimentary sequences acquired from the interpretation of the geological data before interpreting the sedimentary sequence stratigraphy according to the PB-NB boundaries. In other words, the correlation between the INPEFA log curve's turning points and the key stratigraphic boundaries can be ambiguous, inverse, and uncorrelated in some instances and case studies. In the present study, the D-INPEFA Gamma log interpretation was conducted in key well A, which resulted in separating 13 PB-NB boundaries. All valuable software turning points were identified in this manner. Then, the depositional sequence and SB-MFS boundaries identified using cores were presented and boundaries were interpreted based on shifts in the D-INPEFA log (Fig. 10). The findings demonstrated that the actual SB (which correspond to PB-100, PB-400, and PB-600) and MFS (which correspond to NB- 200, NB-400, and NB-600) were similar to the interpretation provided for the correlation of key PB-NB

boundaries with SB and MFS (Table 2). Comparing the key SBs discovered across the interpretation of facies changes and the PB-NB boundaries interpreted via the Gamma log analysis of D-INPEFA revealed that the SB correspond to certain PB surfaces.

It is feasible to characterize the sequence stratigraphy framework in between the studied wells (A -C) merely based on the correspondence of the PB-NB boundaries in other wells. Therefore, it is necessary to establish appropriate correspondence between the key SBs and the significant boundaries recognized through the D-INPEFA chart analysis. In the present study, the key SBs thoroughly corresponded with certain PB-NB boundaries in the three wells of the studied field (Fig. 11). Because of the heterogeneous nature of some reservoirs, employing the D-INPEFA log in the recognized depositional sequences should be done with caution. Nevertheless, studying the sequence stratigraphy of the Fahliyan Formation showed a complete correspondence between the sequences recognized through the cores and the key boundaries derived from the analysis of the D-INPEFA Gamma diagram.

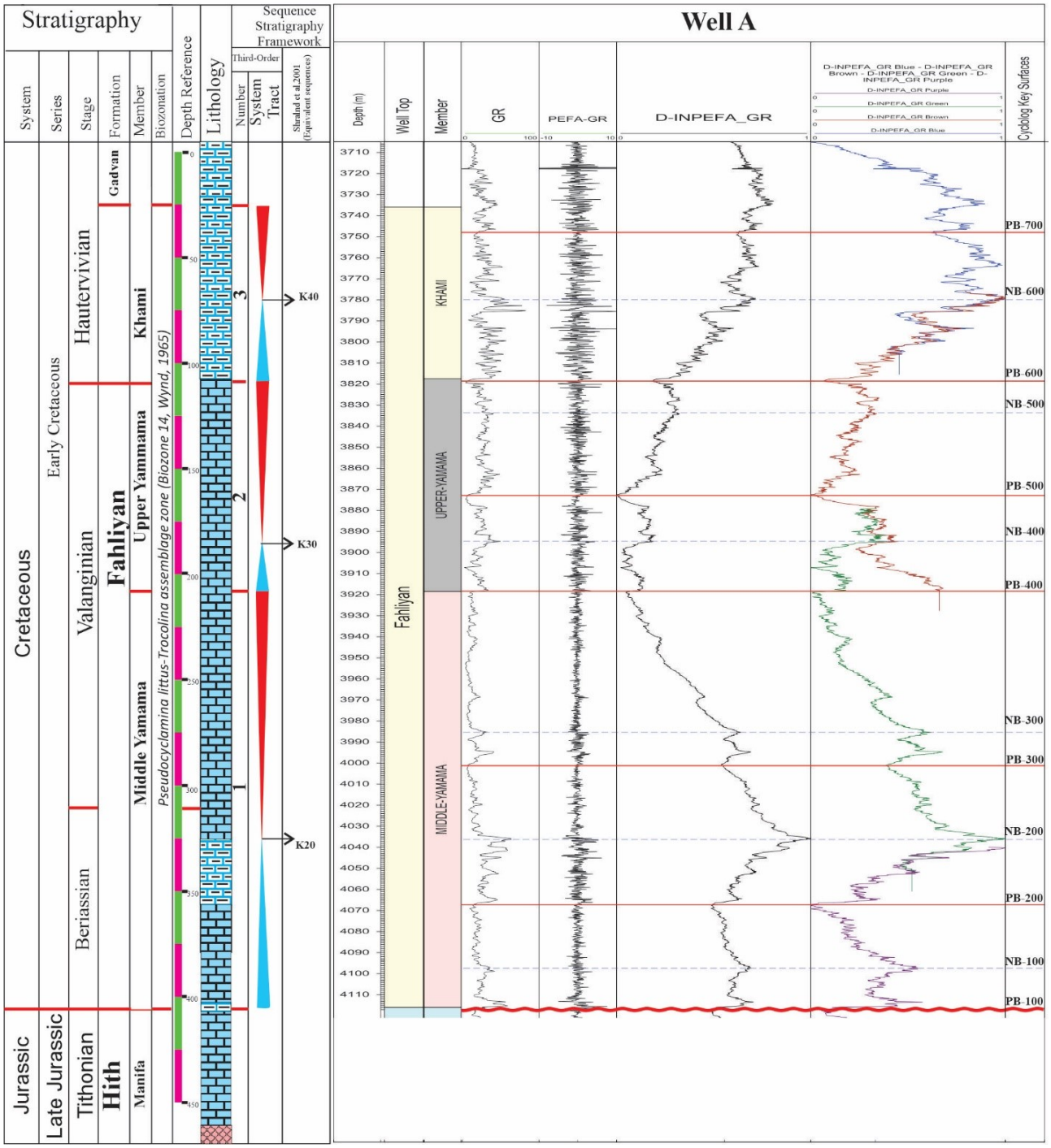

Figure 10. A comparison between the interpretation findings of the D-INPEFA Gamma log with the sequences recognized through core explanation and thin-sections petrography.

Table 2. A comparative analysis of key sequence surfaces and boundaries recognized in the Fahliyan Formation using the D-INPEFA log interpretation; SBs correspond to some PB boundaries, while MFSs correspond to some NB boundaries.

Period	Epoch	Stage	Formation	Third-order Sequences Key Sequence Stratigraphic Surfaces			CycloLog® Stratigraphic Key Surfaces (DINPEFA GR curve)	
				Sequences	SB	MFS	PB	NB
Cretaceous	Early	Hauterivian	Fahliyan	DFS-3	SB-4		PB-700	
						MFS-3		NB-600
					SB-3		PB-600	
		Valanginian		DFS-2		MFS-2		NB-400
					SB-2		PB-400	
		Berriasian-Valanginian		DFS-1		MFS-1		NB-200
					SB-1		PB-100	

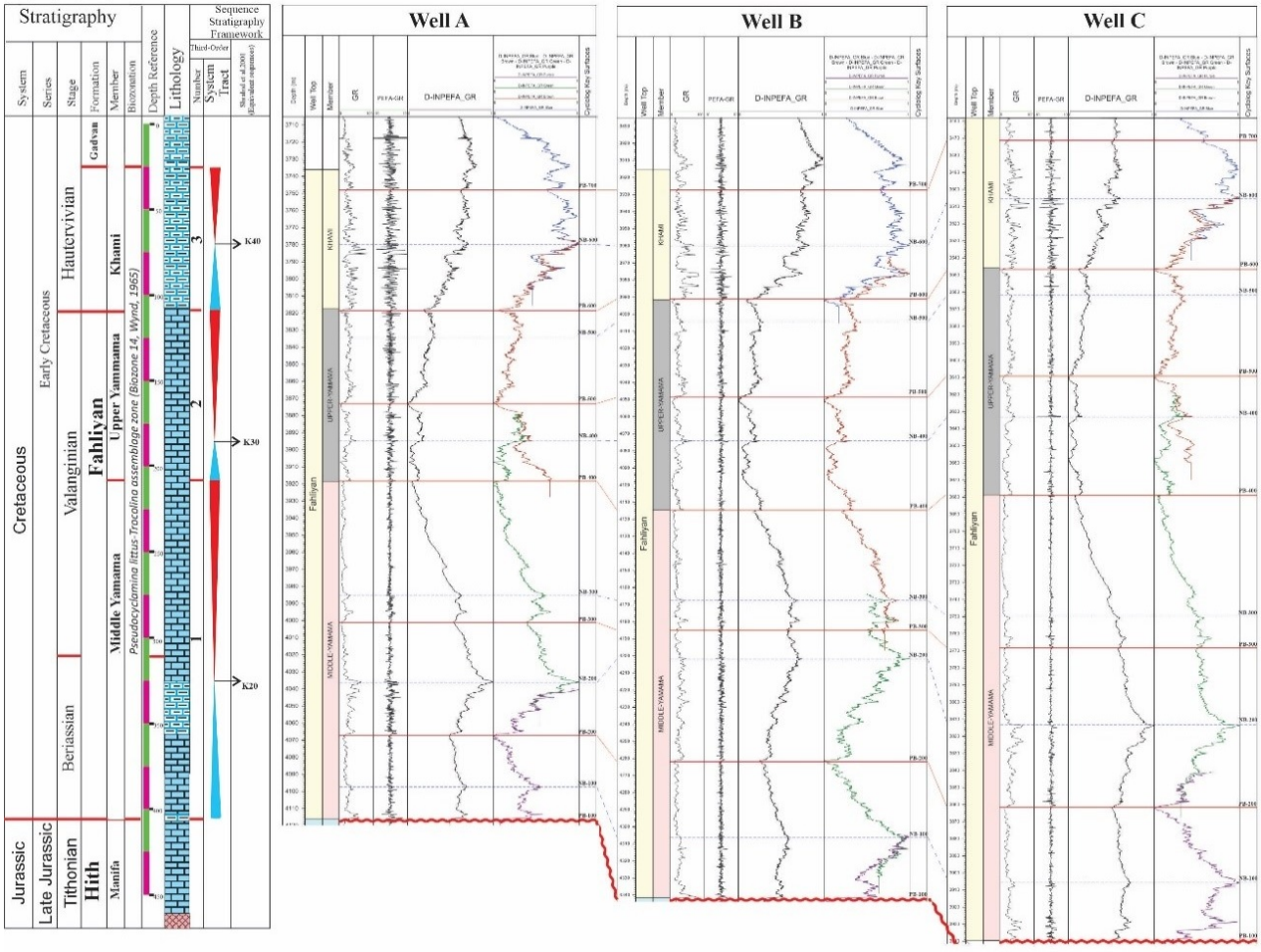

Figure 11. Analysis of the D-INPEFA Gamma chart and NB-PB turning points reveals the correspondence of the identified depositional sequences in the Fahliyan Formation in the investigated field. As can be observed, using the D-INPEFA curve yields satisfactory findings when interpreting sequences using the Gamma log.

5. Conclusion

The present research aimed to investigate the Fahliyan Formation – in an important area of Persian Gulf–to identify facies and interpret its depositional setting and sequence stratigraphy. The main conclusions drawn from this study are as follows:

Integrating core data and petrography of thin sections revealed eight major facies in the intertidal zone, lagoon, shoal, patch reefs, and shallow open marine. The facies were deposited in a carbonate ramp platform considering the gradational facies change in the facies, lack of re-deposited sediments, the absence of extended reef-forming facies, the significant development of grainstone facies, and the comparison with earlier investigations.

Three third-order depositional sequences were identified based on facies changes and the shallowing- and deepening-up pattern of facies. The Jurassic-Cretaceous boundary is defined as the SB at the base of the Fahliyan Formation. This boundary is recognized as an unconformity by some evidence, including karstification and shearing.

The Gamma log was used to evaluate the efficiency of the D-INPEFA in identifying and corresponding sequences. The turning points of the D-INPEFA curve demonstrate a distinct relationship with the SB and MFS. Accordingly, the PB surfaces correspond to the SB in most cases, while the NB surfaces correspond to the MFS. According to the stratigraphic analysis of the Fahliyan depositional sequence, PB-100, PB-400, PB-600, and PB-700 turning points correspond to SB, while NB-200, NB-400, and NB-600 correspond to MFS.

Based on the obtained results, a thorough understanding of the sequence stratigraphy framework could be obtained by interpreting sequence stratigraphy via integrating geological and petrophysical data.

Authors contributions
Authors have contributed equally in preparing and writing the manuscript.

Availability of data and materials
The data that support the findings of this study are available from the corresponding author, upon reasonable request.

Conflict of interests
The authors declare that they have no known competing financial interests or personal relationships that could have appeared to influence the work reported in this paper.

References

Adabi M.H., Salehi M. A., Ghabeishavi A. (2010) Depositional environment, sequence stratigraphy and geochemistry of Lower Cretaceous carbonates (Fahliyan Formation), south-west Iran. *Journal of Asian Earth Sciences* 39 (3): 148–160. DOI: https://doi.org/10.1016/j.jseaes.2010.03.011.

Ahr W. (2008) Geology of carbonate reservoirs: the identification, description and characterization of hydrocarbon reservoirs in carbonate rocks. *Wiley*, 296.

Al-Husseini M.I. (2007) Iran's crude oil reserves and production. *GeoArabia* 12 (2): 69–94.

Bahrehvar M., Mehrabi H., Akbarzadeh S., Rahimpour-Bonab H. (2021) Depositional and diagenetic controls on reservoir quality of the uppermost Jurassic–Lower Cretaceous sequences in the Persian Gulf; a focus on J–K boundary. *Journal of Petroleum Science and Engineering* 201:108512. DOI: https://doi.org/10.1016/j.petrol.2021.108512.

Behdad A. (2019) A step toward the practical stratigraphic automatic correlation of well logs using continuous wavelet transform and dynamic time warping technique. *Journal of Applied Geophysics* 167:26–32. DOI: https://doi.org/10.1007/s40948-016-0027-1.

Catuneanu O. (2006) Principles of Sequence Stratigraphy. *Elsevier,* 375.

——— (2017) Sequence stratigraphy: Guidelines for a standard methodology, In Stratigraphy & timescales. *Academic Press* 2:1–57. DOI: https://doi.org/10.1016/BS.SATS.2017.07.003.

De Jong M., Smith D., Nio S.D., Hardy N. (2006) Subsurface correlation of the Triassic of the UK southern Central Graben: new look at an old problem, first break. 24 (6) DOI: https://doi.org/10.3997/1365-2397.24.1096.26993.

Dickson J. (1966) Carbonate identification and genesis as revealed by staining. *Journal of Sedimentary Research* 36 (2): 491–505.

Esrafili-Dizaji B., Hajikazemi E., Dalvand M., Hassanzadeh Nemati M., Swennen R. (2020) Diagenesis and reservoir characteristics of the Lithocodium–Bacinella facies in a Lower Cretaceous reservoir, eastern Persian Gulf Basin. *Facies* 66 (4): 1–24.

Falahatkhah O., Kordi M., Fatemi V., Koochi H. (2021) Recognition of Milankovitch cycles during the Oligocene–Early Miocene in the Zagros Basin, SW Iran: Implications for paleoclimate and sequence stratigraphy. *Sedimentary Geology* 421:105957. DOI: https://doi.org/10.1016/j.sedgeo.2021.105957.

Flugel E. (2010) Microfacies analysis of Limestones, Analysis Interpretation and Application. Springer:976.

Hassan S., Darwish M., Tahoun S., Radwan A.E. (2022) An integrated high-resolution image log, sequence stratigraphy and palynofacies analysis to reconstruct the Albian–Cenomanian basin depositional setting and cyclicity: Insights from the southern Tethys. *Marine and Petroleum Geology* 137:105502.

Hosseini S., Conrad M.A., Kindler P. (2021) Sequence stratigraphy, depositional setting and evolution of the Fahliyan carbonate platform (Zagros fold-thrust belt, SW Iran) in the Early Cretaceous. *Marine and Petroleum Geology* 128:105062. DOI: https://doi.org/10.22071/gsj.2021.302660.1931.

Hughes G., Naji N. (2008) Sedimentological and micropalaeontological evidence to elucidate post-evaporitic carbonate palaeoenvironments of the Saudi Arabian latest Jurassic. *Volumina Jurassica* 6 (1): 61–73.

Jamalian M., Adabi M. H., Moussavi M. R., Sadeghi A., Baghbani D., Ariyafar B. (2011) Facies characteristic and paleoenvironmental reconstruction of the Fahliyan Formation, Lower Cretaceous, in the Kuh-e Siah area, Zagros Basin, southern Iran. *Facies* 57 (1): 101–122.

Jehangir Khan M., Ghazi S., Mehmood M., Yazdi A., Naseem A.A., Serwar U., Zaheer A., Ullah H. (2021) Sedimentological and provenance analysis of the Cretaceous Moro formation Rakhi Gorge, Eastern Sulaiman Range, Pakistan. *Iranian Journal of Earth Sciences* 13 (4): 252–266. DOI: https://doi.org/10.30495/ijes.2021.1917721.1564.

Kadkhodaie A., Rezaee R. (2017) Intelligent sequence stratigraphy through a wavelet-based decomposition of well log data. *Journal of Natural Gas Science and Engineering* 40:38–50.

Kassem A., Raafat A., Radwan A.E., El Nahas S., Kedzierski M., Zakaria A. (2022) Paleoenvironment, sequence stratigraphy and source rock potentiality of the Cenomanian-Turonian boundary sediments of Southern Tethys. *Marine and Petroleum Geology* 139:105624.

Khalili A., Vaziri-Moghaddam H., Arian M., Seyrafian A. (2021) Carbonate platform evolution of the Asmari Formation in the east of Dezful Embayment, Zagros Basin, SW Iran. *Journal of African Earth Sciences* 181:104229. DOI: https://doi.org/10.1016/j.jafrearsci.2021.104229.

Krassay A. (1998) Outcrop and drill core gamma-ray logging integrated with sequence stratigraphy: examples from proterozoic sedimentary successions of Northern Australia. *Journal of Australian Geology and Geophysics* 17:285–300.

Moghaddasi A., Vaziri-Moghaddam . H, Seyrafian A. (2020) The Maastrichtian-Danian in the SW Zagros Fold-Thrust Belt (S. Iran): An Integration of Planktonic Foraminiferal Biostratigraphy and Gamma-Ray Spectrometry. *Acta Geologica Sinica-English Edition* 94 (5): 1339–1363.

Nio S., Böhm A., Brouwer J., Jong M.D. (2014) Climate Stratigraphy. Principles and applications in subsurface correlation. *European Association of Geoscientists & Engineers,* 134.

Noori H., Mehrabi H., Rahimpour-Bonab H., Faghih A. (2019) Tectonosedimentary controls on Lower Cretaceous carbonate platforms of the central Zagros, Iran: An example of rift-basin carbonate systems. *Marine and Petroleum Geology* 110:91–111.

Rasouli Ghadi P., Sarfi M., Ale Ali S.M., Maleki Z. (2022) The application of GR D-INPEFA Curve in sequence stratigraphy analysis Manifa member and Fahliyan Formation, Northwestern Persian Gulf. *Journal of Earth Science* 32 (3): 119–132.

Sharland P.R., Archer R., Casey D.M., Davies R.B., S.H. Hall, Heward A.P., Horbury A.D., Simmon M.D. (2001) Arabian Plate Sequence Stratigraphy *GeoArabia, Special Publication* 2:371.

Tavakoli V. (2017) Application of gamma deviation log (GDL) in sequence stratigraphy of carbonate strata, an example from offshore Persian Gulf, Iran. *Journal of Petroleum Science and Engineering* 156:868–876.

Van Buchem F.S.P., Simmons M.D., Droste H.J., Davies R.B. (2011) Late Aptian to Turonian stratigraphy of the eastern Arabian Plate–depositional sequences and lithostratigraphic nomenclature. *Petroleum Geoscience* 17 (3): 211–222. DOI: https://doi.org/10.1144/1354-079310-061.

Van Wagoner J., Mitchum R., Campion K., Rahmanian V. (1990) Siliciclastic sequence stratigraphy in well logs, cores, and outcrops: concepts for highresolution correlation of time and facies. *American Association of Petroleum Geologists Special series*

Yong H., Juan X., Wenxiang H., Xiaoyang G. (2021) Application of high frequency lake level change in the prediction of tight sandstone thin reservoir by sedimentary simulation. *Marine and Petroleum Geology* 128:105049. DOI: https://doi.org/10.1016/j.marpetgeo.2021.105049.